

# Balancing uncertainty and complexity to incorporate fire spread in an eco-hydrological model

Maureen C. Kennedy<sup>A,B,E</sup>, Donald McKenzie<sup>C</sup>, Christina Tague<sup>D</sup>  
and Aubrey L. Dugger<sup>D</sup>

<sup>A</sup>University of Washington, School of Environmental and Forest Sciences, Box 352100 Seattle, WA 98195-2100, USA.

<sup>B</sup>Present address: University of Washington, School of Interdisciplinary Arts and Sciences, 1900 Commerce Street, Box 358436, Tacoma, WA 98402, USA.

<sup>C</sup>Pacific Wildland Fire Sciences Laboratory, Pacific Northwest Research Station, US Forest Service, 400 N 34th Street, Suite 201, Seattle, WA, USA.

<sup>D</sup>University of California, Santa Barbara, Bren School of Environmental Science and Management, 2400 University of California, Santa Barbara, CA 93117, USA.

<sup>E</sup>Corresponding author. Email: [mkenn@uw.edu](mailto:mkenn@uw.edu)

**Abstract.** Wildfire affects the ecosystem services of watersheds, and climate change will modify fire regimes and watershed dynamics. In many eco-hydrological simulations, fire is included as an exogenous force. Rarely are the bidirectional feedbacks between watersheds and fire regimes integrated in a simulation system because the eco-hydrological model predicts variables that are incompatible with the requirements of fire models. WMFire is a fire-spread model of intermediate complexity designed to be integrated with the Regional Hydro-ecological Simulation System (RHESSys). Spread in WMFire is based on four variables that (i) represent known influences on fire spread: litter load, relative moisture deficit, wind direction and topographic slope, and (ii) are derived directly from RHESSys outputs. The probability that a fire spreads from pixel to pixel depends on these variables as predicted by RHESSys. We tested a partial integration between WMFire and RHESSys on the Santa Fe (New Mexico) and the HJ Andrews (Oregon State) watersheds. Model assessment showed correspondence between expected spatial patterns of spread and seasonality in both watersheds. These results demonstrate the efficacy of an approach to link eco-hydrologic model outputs with a fire spread model. Future work will develop a fire effects module in RHESSys for a fully coupled, bidirectional model.

**Additional keywords:** HJ Andrews, New Mexico, Oregon, Santa Fe watershed.

Received 9 September 2016, accepted 12 May 2017, published online 30 June 2017

## Introduction

Wildfire affects both the structure and function of watersheds, including rock weathering, modifications to vegetation, microbial and faunal activity, and changes to the soil that affect hydrological processes (Shakesby and Doerr 2006; Hyde *et al.* 2013). In turn, the spatial and temporal patterns of fuels and moisture in a watershed modify fire regimes. These multidirectional influences necessitate the dynamic integration of fire and eco-hydrological modelling, in order to project future watershed processes adequately.

Eco-hydrological models forecast watershed processes and water resources under changing climates and management (Tague and Dugger 2010; Fatichi *et al.* 2016) by combining physical hydrological processes with biological dynamics (Hannah *et al.* 2004; Wood *et al.* 2007). However, disturbance regimes are rarely linked dynamically to eco-hydrological projections, and eco-hydrological models often ignore disturbance

events (Hannah *et al.* 2007). This is problematic, especially for projections of future dynamics, because fires are predicted to become more extensive and severe in many regions (Flannigan *et al.* 2009; Littell *et al.* 2010; Stavros *et al.* 2014). This presents an increasing risk to natural resources, property and ecosystem services (Hurteau *et al.* 2014; Rocca *et al.* 2014).

It is a challenge to integrate a model of fire with an established eco-hydrological model. Eco-hydrological models are not designed from the outset to quantify biomass in a manner compatible with the requirements of the most-used fire models. For example the Regional Hydro-Ecological Simulation System (RHESSys) is an eco-hydrology model that has been applied widely in forested watersheds to estimate streamflow, forest productivity and mortality risk (Tague and Band 2004; Zierl *et al.* 2007; Tague *et al.* 2013a, 2013b; López-Moreno *et al.* 2014). Processes in RHESSys are spatially nested (Fig. 1), and patches are the smallest unit of spatial aggregation. Patches

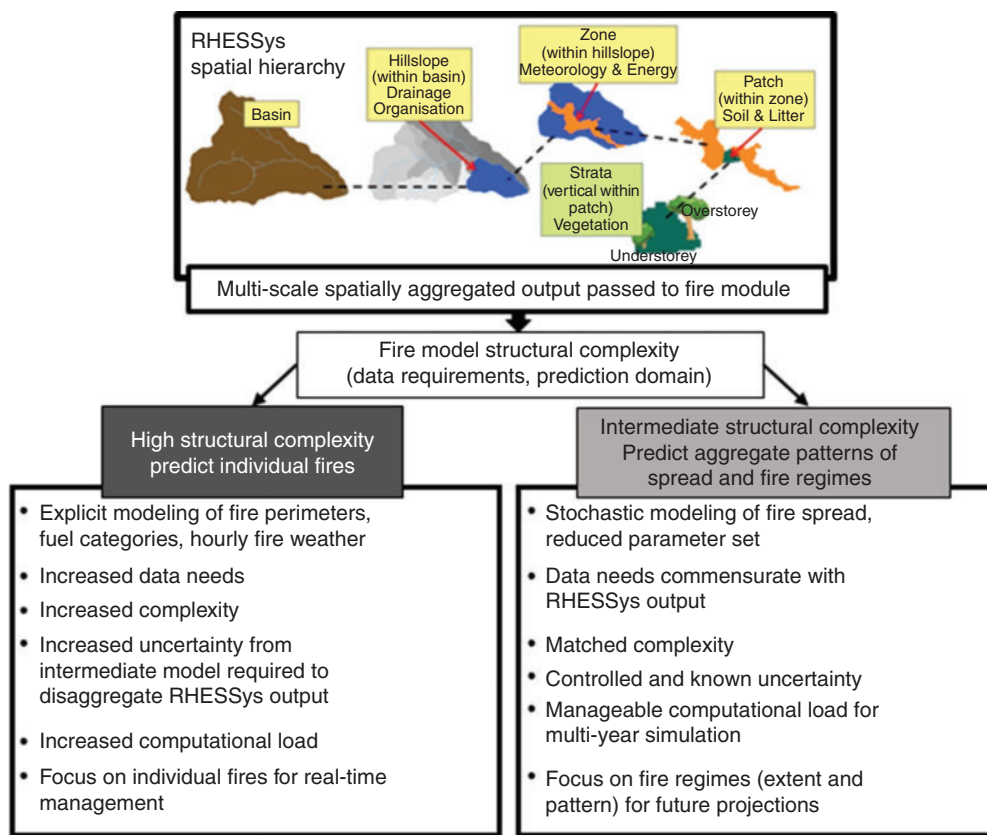


**Fig. 1.** Rationale for a model of intermediate complexity in watershed-scale projections of the effects of climate change on ecosystems (RHESSys, Regional Hydro-Ecological Simulation System, coupled with WMFire). A fire model of high complexity and physical realism introduces extra uncertainty and computational burden when integrated with an existing eco-hydrological model, without increased accuracy (in fact, probably false precision) for longer-term projections. The multiscale RHESSys outputs would have to be collapsed (across scales) and disaggregated (into fuel size classes and fine-scale fire weather) to be used with a structurally complex fire model. Stochastic semimechanistic modelling allows us to match the complexity of the fire module to RHESSys outputs and inputs, thereby minimising uncertainty and focusing on fire-regime characteristics rather than individual fires.

aggregate soil-moisture and land-cover characteristics. Within a patch, there may be canopy strata (vertical layers of biomass that aggregate processes such as photosynthesis and respiration); within these strata, individual organisms (e.g. trees and shrubs) are not simulated. In RHESSys, as in many ecosystem carbon-cycling models (Fatichi *et al.* 2016), biomass components such as leaves and stems are simulated *en masse*, in pools of carbon. This is also true for the litter layer below the canopy strata, which receives input of biomass from the overlaying canopy layers within a patch. The goal of RHESSys, and other similar models of biogeochemical cycling and eco-hydrology, is to simulate ecosystem processes rather than demographics, succession, or competitive interactions (Tague and Band 2004).

If we compare the variables used to describe biomass in RHESSys with the requirements of structurally complex fire models, we see that there is an incompatibility (Fig. 1). For example, semi-empirical models of fire spread that use the Rothermel (1972) equations (e.g. Finney 2004) require specific characteristics of the fuelbed, usually represented by stylised fuel models (Scott and Burgan 2005). Fuel models quantify fuel loading and arrangement by size classes of dead fuels (e.g. litter,

and 1-, 10-, 100-h time lags), live non-woody and woody (herbs, grasses, shrubs) and spatial properties (surface area to volume ratio, fuel bed depth, packing ratio). Because RHESSys does not quantify these fire-relevant properties of biomass, reconciling the mismatch in relevant variables between fire models and eco-hydrological models is not trivial. There are two strategies to couple fire spread with eco-hydrology (Fig. 1): integrate a structurally complex fire model with an adapted eco-hydrological model, or design a fire model of intermediate complexity to integrate with the existing eco-hydrological model.

Integrating a structurally complex fire spread model with the eco-hydrological model requires modifying the eco-hydrological model to predict fire-compatible detailed accountings of fuel loading and arrangement. This has the advantage of increasing physical realism and reducing prediction uncertainty associated with fire spread, if the eco-hydrological model can simulate the detailed fuels accurately. However, detailed descriptions of fuels are not required to simulate hydrological or ecophysiological processes (such as photosynthesis and evapotranspiration), which are the primary objectives of the eco-hydrological model. The outcome of this strategy would be to force a major

re-engineering of the eco-hydrological model, requiring substantial new data sources for calibration and parameterisation, with associated uncertainty in model structure and parameter estimation as well as a substantial increase in computational resources. We believe that modifying the eco-hydrological model to match the requirements of an existing fire model would add uncertainty to the predictions of the fire–eco-hydrological model coupling. The cumulative effect of such uncertainty can be non-linear; for example, a 10% error in parameter estimation can propagate to an order of magnitude greater error in prediction (O'Neill *et al.* 1980).

Furthermore, it is imperative to define the model application niche (the domain over which the model is expected to perform well, and the domain over which model application is not appropriate; Environmental Protection Agency 2009) and to match the level of model structural complexity to the extent and quality of input data (Jackson *et al.* 2000; McKenzie and Perera 2015). The application niche of RHESSys is to predict aggregate patterns in watershed dynamics at time scales of decades to centuries, and how those respond to changes in climate and management. The application niche of RHESSys is not to predict specific events at a given location or time (e.g. timing and location of peak flows following a particular fire). It is therefore sensible that RHESSys does not quantify the specific inputs required by a structurally complex model of fire spread, with an application niche including both the prediction of individual fire events and landscape-level burn probabilities. It is more appropriate to design a fire model of intermediate complexity that better matches the application niche of RHESSys and utilises the existing RHESSys representation of ecosystem and hydrologic variables. Such a model uses the variables of RHESSys to simulate fire in a way that predicts aggregate spatial and temporal patterns of fire spread across the watershed over decades and centuries.

The model WMFire (Kennedy and McKenzie 2017) is designed to accept the inputs of the eco-hydrological model and use them to predict aggregate spatial patterns of fire spread, seasonality, and fire extent and frequency rather than the perimeters and timing of individual fire events. The target application niche of WMFire is to predict a plausible set of outcomes for how fire regimes and fire spread respond to the underlying template of topography, fuels and moisture predicted by the eco-hydrological model. In the present study, we assess a partial coupling of RHESSys and WMFire with the goal to define the application niche of WMFire by elucidating the fire regime characteristics that are predicted adequately and the fire regime characteristics that are not predicted adequately.

#### WMFire model assessment

Model assessment is an iterative process (Reynolds and Ford 1999), and in our ongoing work, we are assessing WMFire in three stages. At each stage, we adapt the approach of Hornberger and Cosby (1985), where traditional statistical analyses of model fit to data are not feasible. The data on historical fire regimes are sparse, with regimes assigned coarse characteristics such as seasonality, severity, frequency and spatial patterns of fire size and spread. We are assessing WMFire against historical fire regimes, without human interference, so recent databases of fire occurrence are not applicable. In the approach

of Hornberger and Cosby (1985), parameter values are identified that produce model results that are considered adequate according to some criterion ('behavioural' in the Hornberger and Cosby (1985) parlance). Uncertainty in parameter values is thereby characterised by the distribution of parameter values able to satisfy the criterion.

In the first stage of WMFire assessment, Kennedy and McKenzie (2017) identified parameter values that were considered adequate to replicate several aggregate spatial statistics of a recent wildfire. In this analysis, they discovered the parameter value associated with fuel moisture had high uncertainty, which led us to improve WMFire to its current version. In the second stage of model assessment (presented here), we evaluate a partial integration of WMFire with RHESSys to assess the ability of WMFire to use RHESSys model outputs to adequately satisfy several criteria associated with historical fire regimes for two watersheds (HJ Andrews watershed in Oregon, USA (HJA), and Santa Fe watershed in New Mexico, USA (SF); Fig. 2). This stage of model assessment does not incorporate fire effects for two main reasons. The fire effects module for RHESSys is still under development, and in this second stage of assessment, we want to isolate the uncertainties associated with the fire spread model before assessing the full integration with RHESSys including fire effects (to be completed in the third stage of model assessment). Through each stage of model assessment, we are able to characterise the application niche of the model integration.

## Methods

### Study sites description

The upper Santa Fe River watershed (Table 1) is the water supply catchment for Santa Fe, New Mexico. It is a steep, largely forested watershed with elevations ranging from 2300 to 3800 m. Dominant vegetation is ponderosa pine at lower elevations (hereafter PP), mixed conifer (Douglas-fir, ponderosa pine, white pine, quaking aspen; hereafter MC) at mid-elevations, and spruce-fir (Engelmann spruce dominant) at higher elevations. Mean annual precipitation is  $\sim 700$  mm year<sup>-1</sup> (at the mid-elevation Elk Cabin SNOTEL station), including summer monsoonal rainfall input and winter snowfall. The HJ Andrews watershed (Table 1) is located in the Western Oregon Cascade Range. Elevation ranges from 430 to 1600 m. The watershed is a mixed-conifer forest dominated by Douglas-fir and western hemlock. Mean annual precipitation is 2200 mm year<sup>-1</sup> and falls primarily during the winter months, largely as rain at the lowest elevations and snow at the highest elevations.

### RHESSys study site calibrations

As with most watershed-scale hydrologic models, in RHESSys, subsurface drainage parameters usually need to be calibrated by comparison of modelled with observed streamflow using observed historical weather and climate data (Tague *et al.* 2013a; Garcia and Tague 2015). The implementation and calibration of RHESSys for SF has not been previously published; this calibration is described in Supplementary material. The implementation and calibration of RHESSys for HJA used in the present study is described in Garcia *et al.* (2013), and summarised in the Supplementary material.



**Fig. 2.** Location of the two study sites, HJ Andrews in Oregon, and the Santa Fe Watershed in New Mexico, and topography and spatial distribution of litter fuel loads ( $\text{kg m}^{-2}$ ) predicted by RHESSys (Regional Hydro-Ecological Simulation System) for each watershed, given as a pixel-wise mean value across all years in the simulation.

**Table 1.** Characteristics of the study sites including expected fire regimes

Area is that of each watershed. Expected fire regime characteristics for Santa Fe (SF) and HJ Andrews (HJA) are based on published fire histories for each site

	Area (ha)	Elevation	Annual precipitation	Criterion 1: spatial gradient fire occurrence	Criterion 2: seasonality of fire occurrence	Criterion 3: fire frequency occurrence
SF	7559	2300 to 3800 m	700 mm year <sup>-1</sup>	Increasing from lower to middle watershed, then decreasing in lower watershed	May–July	4.3–31.6 years (fire return interval)
HJA	6175	430 to 1600 m	2200 mm year <sup>-1</sup>	No spatial gradient	August–September	50–200 years (natural fire rotation)

*Historical fire regime characteristics at each site*

We use published fire history data and the LANDFIRE fire regime group geospatial layer (LANDFIRE 2014; Figs S1 and S2) to characterise observed patterns in fire regime characteristics for each watershed. LANDFIRE is a project of multiple US federal agencies to produce data layers of landscape vegetation, fuels and fire regimes. In SF, Margolis and Balmat (2009) report mean fire return intervals between 4.3 and 31.6 years (Table 1) depending on how many scars are used to indicate a fire and whether the fire is recorded in the PP or MC zone (Margolis and Balmat 2009). Among the fire scars for which season could be determined, most were in the beginning of the growing season (May–June). In the higher-elevation spruce forest, they found evidence for one stand-replacing fire in 1685. Therefore, a fire event in that portion of the watershed would not necessarily be expected over the simulation period. These patterns are corroborated by the LANDFIRE fire regime group data

layer (see Fig. S2), where there is a low–mixed-severity fire regime inferred for the lower to middle watershed with mean fire return intervals  $\leq 35$  years, or 35–200 years depending on location (Fig. S2; Table S2). LANDFIRE also predicts stand-replacement fire severity in the upper SF watershed.

For HJA, fire history studies and LANDFIRE document a mixed- or high-severity fire regime, with few small fires and the occasional large stand-replacing fire (Teensma 1987; Weisberg 1998; LANDFIRE 2014). The fire-return interval is of the order of decades to centuries, with a natural fire rotation ranging from ~50 to ~200 years (Tables 1, S2; Fig. S1). Therefore, over the period for the simulation (50 years), we would expect at most one large fire for a single realisation, regardless of whether fire effects are included in the model simulation. In mixed-severity fire regimes such as HJA, fires more likely occur later in the growing season, as the fuels dry throughout the summer (Bartlein *et al.* 2008).



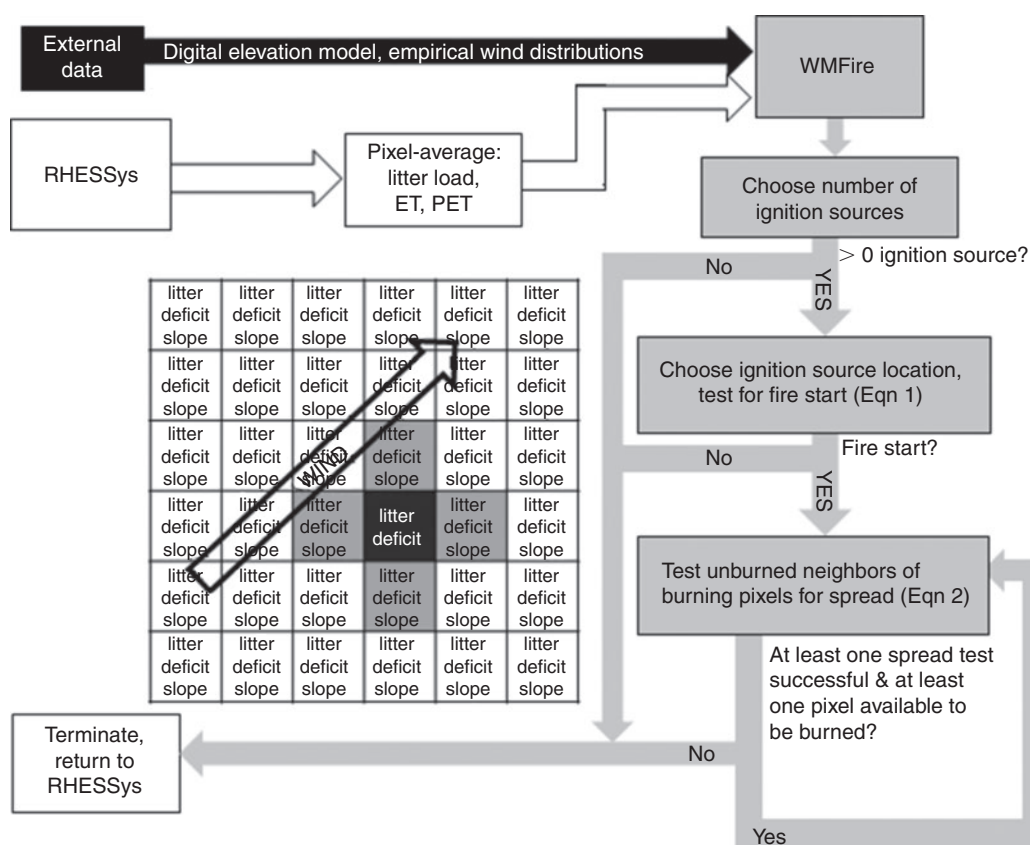


Fig. 3. Flow diagram for WMFire fire spread (ET and PET, actual and potential evapotranspiration).

The documented fire history and LANDFIRE fire regime groups determine assessment criteria for this stage of WMFire assessment. For SF, the criteria are (Table 1):

- SF1. Spatial gradient in fire size and occurrence from the lower to upper watershed
- SF2. Fire spread peaks in May–July
- SF3. Fire-return interval 4.3–31.6 years

For HJA, the criteria are (Table 1):

- HJA1. No spatial gradient in fire size and occurrence
- HJA2. Fire spread peaks in July–September
- HJA3. Natural fire rotation 50–200 years.

#### WMFire–RHESSys description

Each month, RHESSys calculates the monthly mean for litter carbon load ( $\text{kg m}^{-2}$ ), and actual and potential evapotranspiration (ET and PET respectively;  $\text{mm m}^{-2} \text{ day}^{-1}$ ; Stephenson 1998), then passes those values as well as the digital elevation model to WMFire (Fig. 3). (Note: RHESSys computes these values daily but we aggregate to a monthly time step as a compromise between allowing for submonthly changes in fire season, and the computational burden of running WMFire.) Details on RHESSys estimates of litter carbon, ET and PET can be found in Tague and Band (2004). As a surrogate for fuel moisture, WMFire calculates the relative moisture deficit,  $1 - \text{ET}/\text{PET}$  (Swann *et al.* 2012; Kennedy and McKenzie 2017).

Given that our goal is to predict plausible futures rather than specific events, and that fire is driven by stochastic processes such as weather events, we designed WMFire to be a stochastic model that subsumes in the probability calculation the uncertainty associated with the natural variability in fire events. When WMFire is called, the following sequence of events occurs (Fig. 3), described in more detail below:

- (1) Draw a random number of ignition sources. If this number is greater than 0, locate each ignition source randomly on the landscape.
- (2) For each ignition source located randomly on the landscape, test the chosen pixels for fire start based on the fuel and moisture conditions of the pixel.
- (3) For each successful fire start, simulate fire spread based on the fuel, moisture, topographic and wind conditions.
- (4) Return to RHESSys which pixels, if any, were burned during the simulation.

#### Ignition sources

A successful fire ignition occurs when two events happen in sequence: first, there is an ignition source located on a landscape (such as lightning, campfires), then that ignition source successfully ignites a wildfire. Although the instance of an ignition source that successfully starts a wildfire is observable, observations of ignitions that do not lead to wildfires are severely limited. Thus, the full sample space of ignition source rates,

**Table 2.** WMFire parameter values and empirically estimated wind coefficients for both the Santa Fe (SF) and HJ Andrews (HJA) watersheds

$k_{1\_load}$  controls the steepness of the probability of spread with increasing litter load;  $k_{2\_load}$  defines the litter load ( $\text{kg m}^{-2}$ ) at which the associated probability of spread crosses a value of 0.5;  $k_{1\_def}$  controls the steepness of the probability of spread with increasing relative deficit ( $1 - \text{ET}/\text{PET}$ , where ET is evapotranspiration and PET is potential evapotranspiration);  $k_{2\_def}$  defines the relative deficit at which the associated probability of spread crosses a value of 0.5;  $k_{1\_wind}$  controls the wind direction at which the associated probability falls below 1;  $k_{2\_wind}$  gives the associated probability of spread against the wind direction;  $k_{1\_slope}$  gives the associated probability of spread on a flat slope;  $k_{2\_slope}$  controls the steepness of the probability of spread with increasing or decreasing slope;  $\lambda$  is the mean ignition source rate (per month)

WMFire parameters	$k_{1\_load}$	$k_{2\_load}$	$k_{1\_def}$	$k_{2\_def}$	$k_{1\_wind}$	$k_{2\_wind}$	$k_{1\_slope}$	$k_{2\_slope}$	$\lambda$
SF and HJA	3.9	0.07	3.8	0.27	0.87	0.48	0.91	1.0	HJA: 0.1, 0.25, 0.5 SF: 1, 1.5, 2

those that both do and do not result in a wildfire, is essentially unobservable. Adherence of ignition source rate to a particular historical frequency of ignition sources (for which there are few reliable data sources) introduces false precision into simulations and ignores the high uncertainty in determining ignition sources on a landscape. Even if ignition rates are known, they are poor predictors of area burned at almost any scale (Krause *et al.* 2014; Faivre *et al.* 2016).

In WMFire, we compute a successful fire ignition as a function of the ignition source rate and the probability that a given ignition leads to a fire. The latter variable is a function of landscape and climatic variables that can be readily computed by RHESys (described in detail below). As noted above, the lack of observable data limits the development of predictive models of ignition source rates. Given this uncertainty, for WMFire, we assume a simple mean rate of ignition sources ( $\lambda$ ), informed by the area of the watershed (a larger watershed is given a larger ignition source rate). The number of ignition sources to be tested for fire start is drawn from a Poisson distribution, with the ignition source rate as the Poisson rate parameter. Given that data are not available for the ignition source rate, we conduct a local sensitivity analysis on the mean ignition source rate for each watershed (0.10, 0.25 and 0.5 mean ignition sources per month for HJA, and 1, 1.5 and 2 mean ignition sources per month for the larger SF watershed; Table 2).

#### Test for fire start

A random pixel in the watershed is chosen for each ignition source to test for successful fire start. In WMFire, the probability of a successful ignition ( $p_i$ ), given the presence of an ignition source, depends on the RHESys predicted values of litter load ( $l$ ) and relative deficit ( $d$ ). First, individual probabilities are calculated associated with each variable ( $p_i(l)$ ,  $p_i(d)$ ; described below), then the final probability of successful ignition is the product of the component probabilities:

$$p_i(l, d) = p_i(l) \times p_i(d) \quad (1)$$

#### Fire spread given successful fire start

The spread model in WMFire is based on a system of dynamic percolation (Caldarelli *et al.* 2001; Kennedy and McKenzie 2010; McKenzie and Kennedy 2012). The basic sequence of fire spread is (Fig. 3): if an ignition source successfully ignites a pixel, then WMFire tests the orthogonal neighbours of that pixel against the probability of spread ( $p_s$ )

independently. For each pixel to which spread is successful, spread to each of its neighbours is tested in the next iteration. Previously burned pixels can no longer spread fire.

In WMFire, the value of  $p_s$  is determined by the RHESys-predicted value of litter load ( $l$ ), relative deficit ( $d$ ), topographic slope ( $S$ ) and the orientation of spread relative to wind direction ( $w$ ). A probability associated with each of those components is calculated ( $p_s(l)$ ,  $p_s(d)$ ,  $p_s(S)$  and  $p_s(w)$  for the probability of spread associated with fuel load, deficit, slope and wind respectively). The final probability of spread ( $p_s(l, d, S, w)$ ) is calculated as the product of the component probabilities:

$$p_s(l, d, S, w) = p_s(l)p_s(d)p_s(w)p_s(S) \quad (2)$$

In this formulation, if any of the components predicts a probability of zero for spread (is a barrier to spread), then spread cannot happen. Conversely, if all components predict a probability of 1 for spread (no barriers to spread), then spread will happen. Next, we describe how each component probability for fire start and fire spread is calculated.

#### Litter load and relative deficit

We assume that the probability associated with litter load and relative deficit increases with increasing values of each of those, and this relationship takes a sigmoid shape. The function that associates  $p_s$  and  $p_i$  with litter load ( $l$ ) and relative deficit ( $d$ ) takes the form:

$$p_s(l) = \frac{1}{1 + e^{-k_1 l (l - k_2 l)}} \quad (3)$$

$$p_s(d) = \frac{1}{1 + e^{-k_1 d (d - k_2 d)}} \quad (4)$$

where  $k_1$  defines the shape of the curve (its steepness),  $k_2$  defines where along the  $x$  axis the function crosses a value of 0.5 (Fig. 4a, b; Table 2), which is near the value of the percolation threshold estimated for this kind of dynamic percolation (Kennedy and McKenzie 2010).

#### Wind

We assume that the probability of fire spread is highest in the wind direction, then decreases as the angle of spread deviates from the wind direction. We adapt a trigonometric function used by Weisberg *et al.* (2008):

$$p_s(w) = k_{1\_wind}(1 + \cos(\gamma - \omega)) + k_{2\_wind} \quad (5)$$

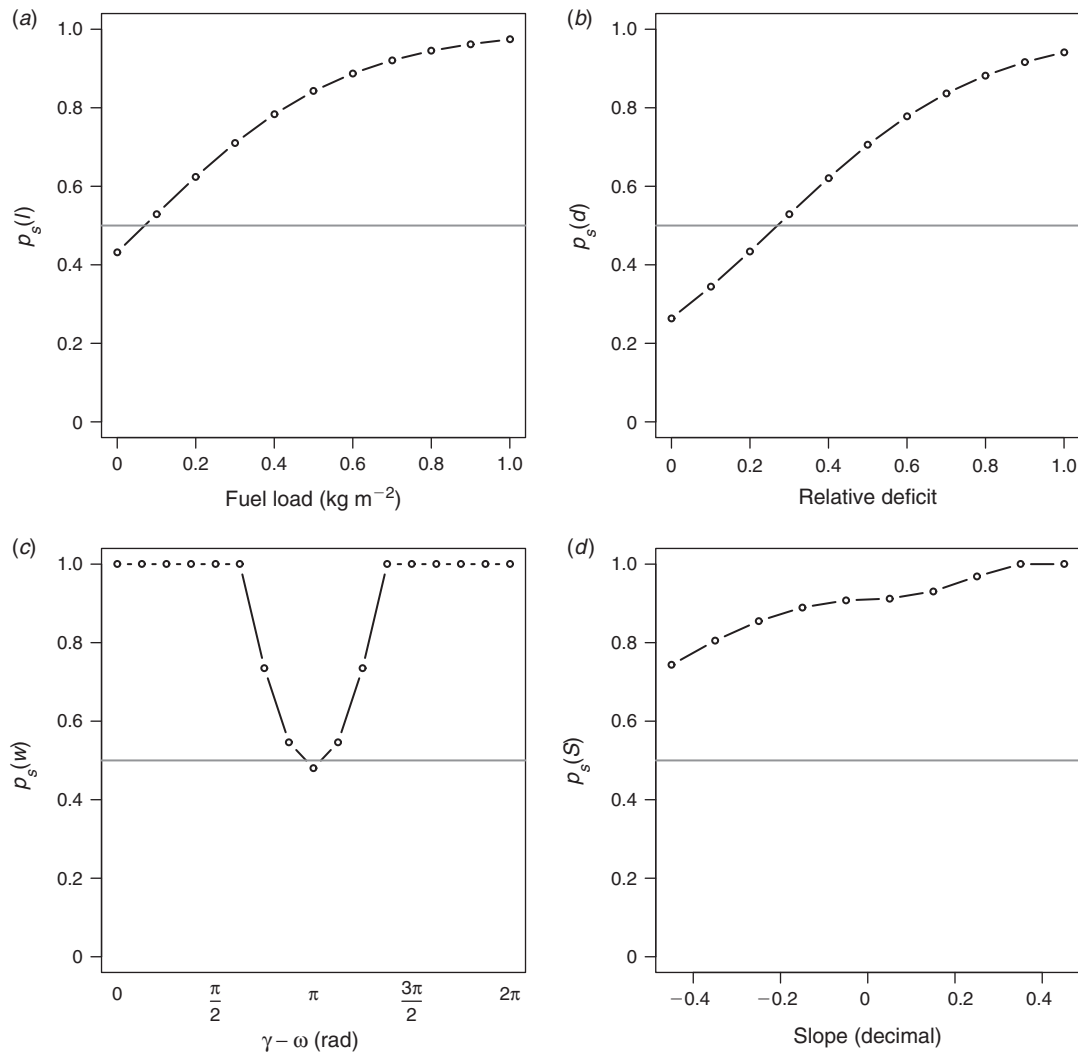


**Fig. 4.** Function shapes for WMFire at the chosen parameter values. (a) Fuel load; (b) relative moisture deficit; (c) wind direction relative to spread direction; (d) slope relative to spread direction. Horizontal line at probability of spread  $p_s = 0.5$ .

where  $k_{1\_wind}$  controls the reduction of  $p_s(w)$  as the angle of spread deviates from the wind direction,  $\omega$  is the wind direction (rad),  $\gamma$  is the orientation of the neighbour pixel relative to the pixel spreading fire (rad) and  $k_{2\_wind}$  is the probability of spread against the direction of the wind (Fig. 4c; Table 2). This function can take values  $>1.0$ , in which case  $p_s(w)$  is set to 1. The empirical modelling of wind distributions is described in the Supplementary material.

#### Slope

The probability of fire spread increases uphill and decreases downhill from the source pixel. We adapt our curve from the model LANDSUM (Keane *et al.* 2002):

$$p_s(S) = k_{1\_slope} e^{I k_{2\_slope} S^2} \quad (6)$$

where  $k_{1\_slope}$  gives the value of  $p_s$  at zero slope,  $k_{2\_slope}$  defines the steepness of the curve, and  $I = 1$  if  $S > 0$ ,  $-1$  otherwise (Fig. 4d; Table 2). This function can take values  $>1.0$ , in which

case  $p_s(S)$  is set to 1. The slope relative to the direction of fire spread is calculated from the digital elevation model (DEM).

#### WMFire parameter values

The values of the eight WMFire parameters were selected by continuing the first assessment procedure described by Kennedy and McKenzie (2017), and the chosen values are given in Table 2. Note that the parameter values for  $p_s(l)$  and  $p_s(d)$  are the same as those for  $p_s(l)$  and  $p_s(d)$ .

#### Assessing WMFire against criteria

To assess the fire spread model, we generate RHESSys-predicted grids of mean monthly fuel load and mean monthly relative deficit over the historical period for each watershed. These are used as a time series of input grids for WMFire, along with the DEM and the empirical wind distributions (Fig. 3). We conducted 500 Monte Carlo (MC) replicate simulations for each time series of deficit and load, resulting in 300 000 total WMFire calls for HJA and 396 000 for SF. For all fire regime

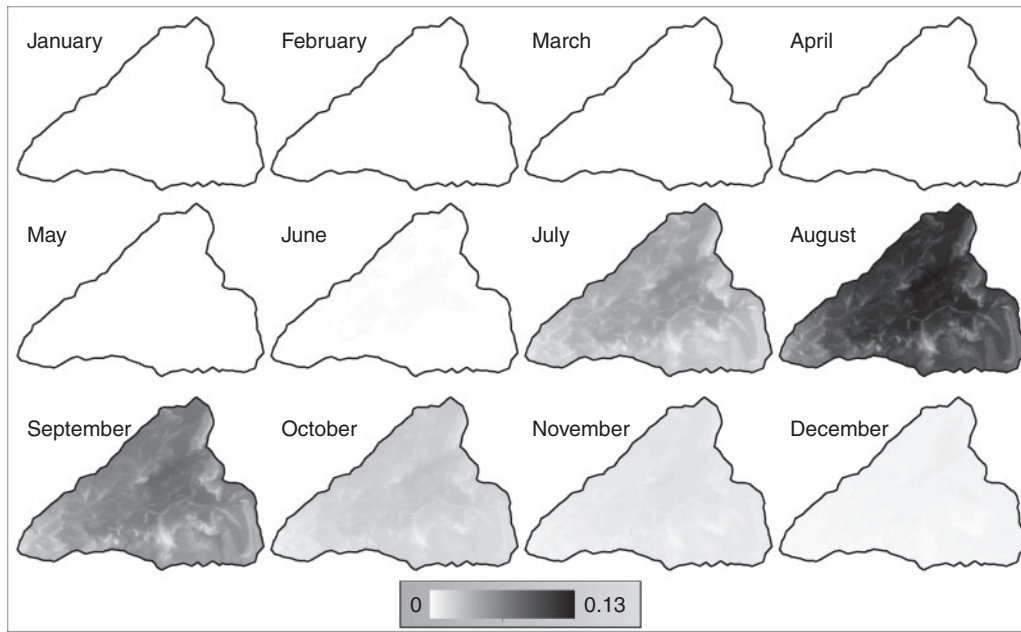


**Fig. 5.** Proportion of replicates (prop reps) where model simulates fire in each pixel across all years, calculated as the proportion of times each pixel experiences fire relative to the number of ignitions tried (reps  $\times$  years) for HJ Andrews (HJA) with an ignition rate of 0.5 per month. Note different scales for [Figs 5 and 6](#).

characteristics, we count fire spread both at a threshold of successful ignition ( $>0$  ha burned) and at a threshold of minimum successful spread ( $>100$  ha burned). We chose the first threshold to represent any successful start, then the second threshold to represent successful spread given fire start. The 100-ha threshold is fairly arbitrary, but we believe sufficient for the purpose of comparing simulations with fire history data where fire size is difficult to determine.

To assess the spatial distribution of fire spread (criterion 1 for each watershed), we determine pixel-level probabilities of fire activity by calculating, for each month, the proportion of times an individual pixel experiences fire across replicate simulations. We then create maps of those probabilities and compare the patterns with the criterion for each watershed ([Table 1](#)).

To assess the seasonality of fires in the regime (criterion 2 for each watershed), we calculate the proportion of replicates that experience fire ( $>0$  ha burned or  $>100$  ha burned) each month through all simulation years. We then compare the maximum month of fire occurrence with the criterion for each watershed ([Table 1](#)). We also record fire sizes to characterise the simulated fire size distribution.

To compare against the third criterion for each watershed, we calculate the fire-return interval, the mean number of years between fires ( $>0$  ha burned and  $>100$  ha burned) for each replicate simulation. The **natural fire rotation (NFR;** [Heinselman 1973](#)) is also calculated for each replicate.

$$\text{NFR} = \frac{A_s}{\bar{A}} \quad (7)$$

where  $A_s$  is the total area of the watershed and  $\bar{A}$  is the mean annual area burned throughout the individual time series

([Swetnam \*et al.\* 2011](#)). We then compare the distributions of fire return interval and NFR with the criterion for each watershed ([Table 1](#)).

## Results

Empirical wind distributions and RHESSys-predicted values of litter load and relative deficit for each watershed are given in the Supplementary material ([Table S1](#), [Figs S3, S4](#)). Here, we focus on comparing WMFire predictions with the assessment criteria for each watershed, which are derived from site-specific literature and LANDFIRE data, and are listed in [Table 1](#).

### *Criterion 1: spatial distribution of fire spread*

Simulated pixel-wise probabilities of fire in SF increase from the lower to the middle watershed, then decline in the upper portion of the watershed ([Fig. 5](#)), and this spatial pattern is not sensitive to the ignition source rate ([Figs S8–S10](#)). This spatial pattern satisfies criterion SF1 ([Table 1](#)). Simulated pixel-wise probabilities of fire in HJA do not show an obvious spatial gradient, although there is patchiness in fire probability ([Fig. 6](#)). These spatial patterns are not sensitive to the ignition source rate ([Figs S5–S7](#)), and satisfy criterion HJA1.

### *Criterion 2: seasonality of fire occurrence*

For SF, the proportion of replicates that achieve a fire size  $>100$  ha shows a distinct seasonality, with a peak in June. All months show a small probability of fire activity, but most activity is in the months May–July ([Fig. 7](#)). This pattern in seasonality of fire spread is not sensitive to the value of ignition source rate ([Figs S8–S10](#)), and it satisfies criterion SF2. The value of the proportion of successful fire is sensitive to the mean



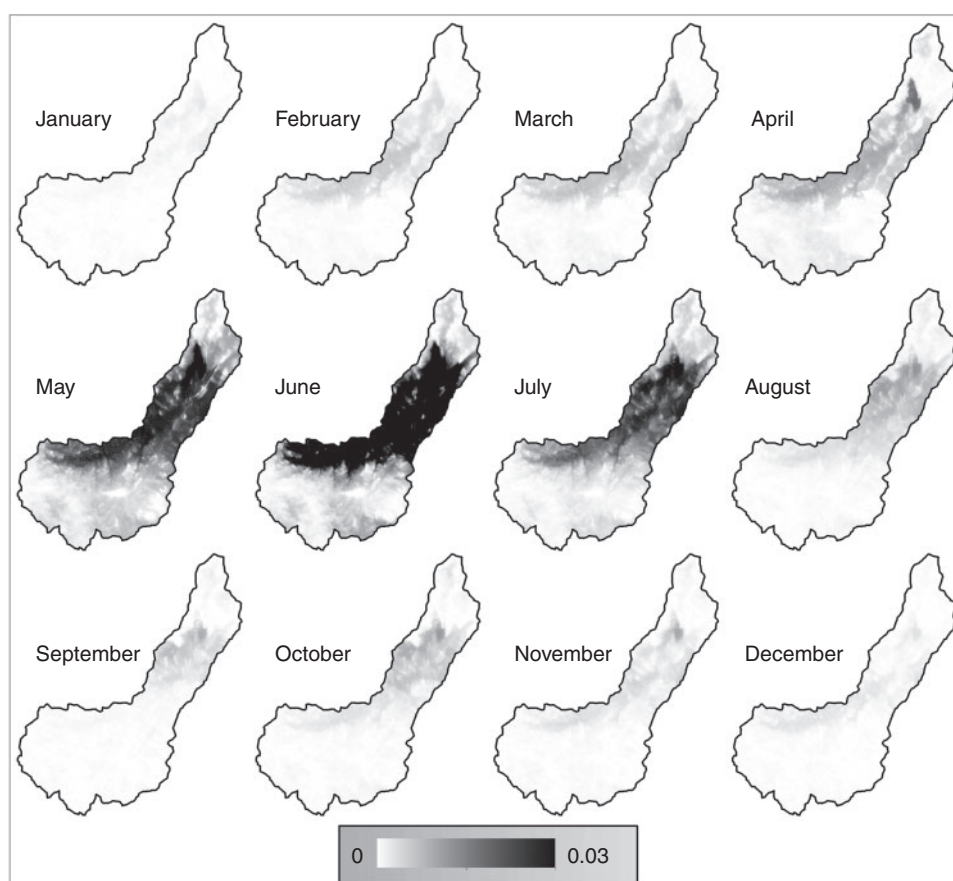


**Fig. 6.** Proportion of replicates (prop reps) where model simulates fire in each pixel across all years, calculated as the proportion of times each pixel experiences fire relative to the number of ignitions tried (reps  $\times$  years) for Santa Fe (SF) with an ignition rate of 2 per month. Note different scales for Figs 5 and 6.

ignition source rate. WMFire predicts that fire activity for HJA increases as the growing season progresses, peaking in the late summer and early fall (autumn) (Fig. 7). In the HJA, fire is predicted to be absent in the late winter and early spring months, and it rarely occurs in the late fall and early winter. This pattern in seasonality of fire spread is not sensitive to the value of ignition source rate (Figs S5–S7), and it satisfies criterion HJA2. The value of the proportion of successful fires in HJA is sensitive to ignition source rate, and it is near zero when the ignition source rate is 0.1 per month.

#### Criterion 3: fire return interval

In both watersheds, metrics of fire return are sensitive to the mean ignition source rate. For respective mean ignition source rates of 1, 1.5 and 2 per month, in SF the mean values of NFR are 84.3, 54.5 and 40.9 years; the mean return interval for successful ignition is 1 year for all mean ignition source rates; the mean return intervals for fires that achieve a size at least 100 ha are 9.1, 6.5 and 5.2 years (Fig. 8). For all tested mean ignition source rates, criterion SF3 is satisfied. For respective mean ignition source rates of 0.1, 0.25 and 0.5 per month, in the smaller HJA watershed, the mean values of NFR are 314 431.9, 9.9 and 4.6 years; the return intervals for successful ignition are 13.6, 1.4 and 1.1 years; the mean values for return intervals for fires

>100 ha are 19.3, 4.4 and 2.5 years (Fig. 8). The closest match between model prediction and criterion HJ3 is for a mean ignition source rate of 0.1 per month.

#### Fire size distribution

For fires that attain at least 100 ha, the distributions of fire sizes are right-skewed (Fig. 8) in SF. The largest fires occur in the early summer fire season. The fire-size distribution in HJA is fairly symmetric. Maximum fire sizes are slightly larger in HJA than in SF, with more fires achieving the larger fire sizes (Fig. 8).

#### Discussion

By matching the level of complexity and application niche of RHESys, WMFire is able to satisfy the first two assessment criteria (spatial distribution of fire spread and seasonality of fire occurrence) when compared with documented fire histories for HJA and SF (Figs 5–6; Table 1). The ability of WMFire to satisfy these two criteria is not dependent on the value of the ignition source rate (Figs S5–S10).

#### WMFire application niche

For SF, WMFire predicts a peak in fire spread during the late spring and early summer, which is expected given the fire

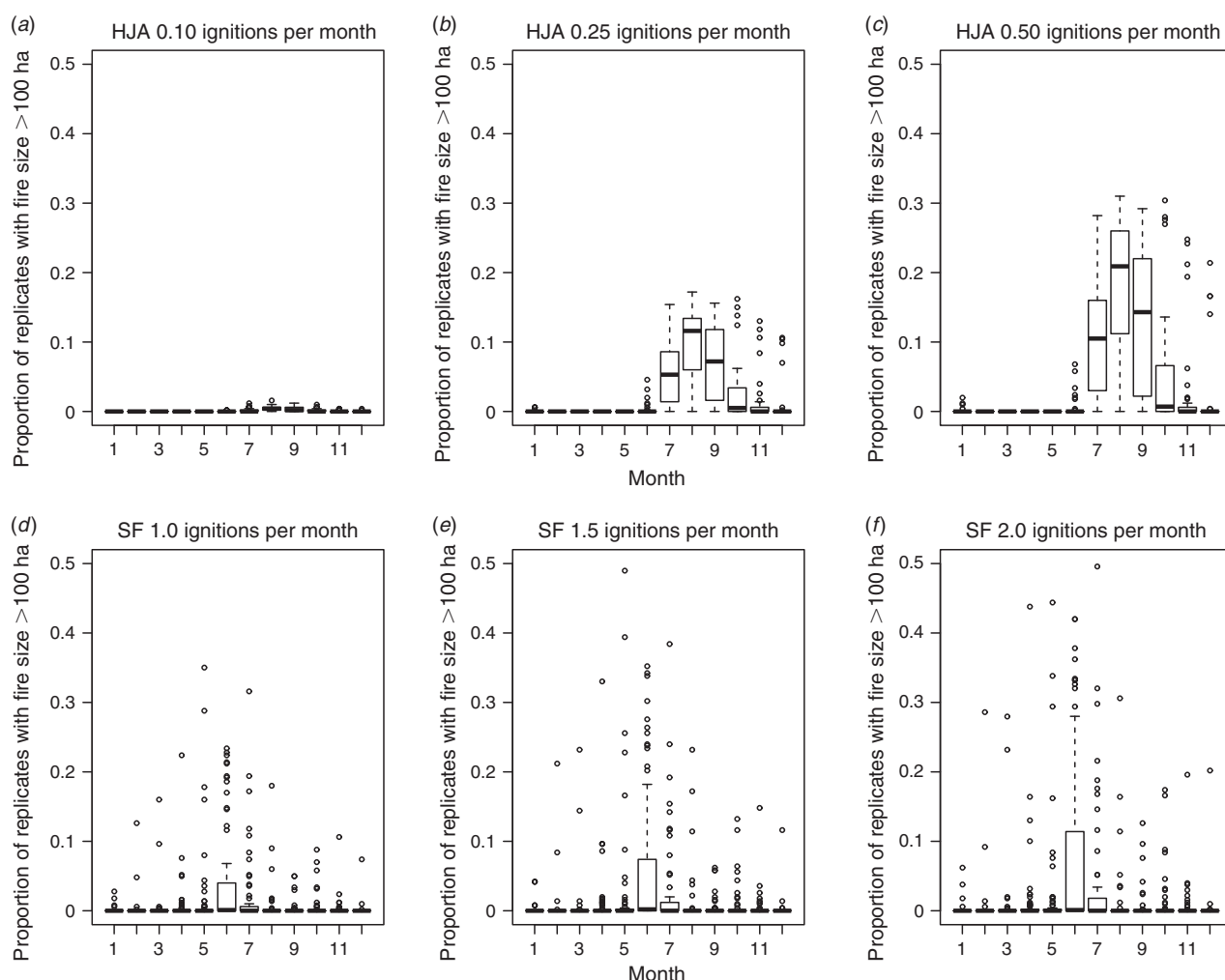


**Fig. 7.** Proportion of replicates with fire size > 100 ha each month. Sources of variability are years and replicates. (a–c) HJ Andrews (HJA) ignition rates of 0.10, 0.25 and 0.5 per month. Peak fire activity is predicted in the late summer and early fall months. (d–f) Santa Fe (SF) ignition rates of 1, 1.5 and 2 per month. Peak fire activity is predicted in the late spring and early summer months.

history recorded for that watershed (Margolis and Balmat 2009; LANDFIRE 2014). For HJA, WMFire predicts a peak in fire spread during the late summer, also consistent with the observations of fire history in that watershed (Teensma 1987; Weisberg 1998; LANDFIRE 2014). These observed patterns in historical seasonality are not sensitive to the value of ignition source rate, indicating that there is little uncertainty in the seasonality of fire spread predicted by WMFire.

For SF, WMFire predicts a spatial gradient where the highest density of fire occurrence is in the middle portion of the watershed. This pattern matches the fire history data (Margolis and Balmat 2009) and LANDFIRE predictions (Fig. S2; Table S2). LANDFIRE predicts that the lowest return intervals (and thereby the greatest expected fire occurrence) are in the lower to the middle portion of the watershed, and fire history data show that the middle portion of the watershed is expected to have a mixed-severity fire regime.

The simulated fire size distribution in SF is right-skewed and heavy-tailed (Fig. 8), which follows other estimated empirical

fire size distributions (Malamud *et al.* 2005). The simulated fire size distribution in HJA shows larger values and is more symmetric, implying that when a fire does burn in HJA, it tends to be large, and smaller fire sizes are rare (Fig. 8). LANDFIRE predicts a mixed to high-severity fire regime for HJA, which is expected to have larger fires of higher severity than SF. For any individual fire simulated in HJA, the spread pattern follows what is expected in this fire regime – a fairly large fire supported by high relative deficits and fuel loading (Teensma 1987; Weisberg 1998; Fiorucci *et al.* 2008). This is consistent with WMFire predictions of fire size for HJA. The fire size distribution in both watersheds is not sensitive to the ignition source rate, indicating that there is little uncertainty in the fire size distribution predicted by WMFire.

In this stage of model assessment, we find that the outcomes of successful ignitions – fires that spread, their seasonality and extent – are metrics of the fire regime for which our current model structure is adequate. However, sensitivity analysis of ignition source rate shows that the ability of WMFire to satisfy

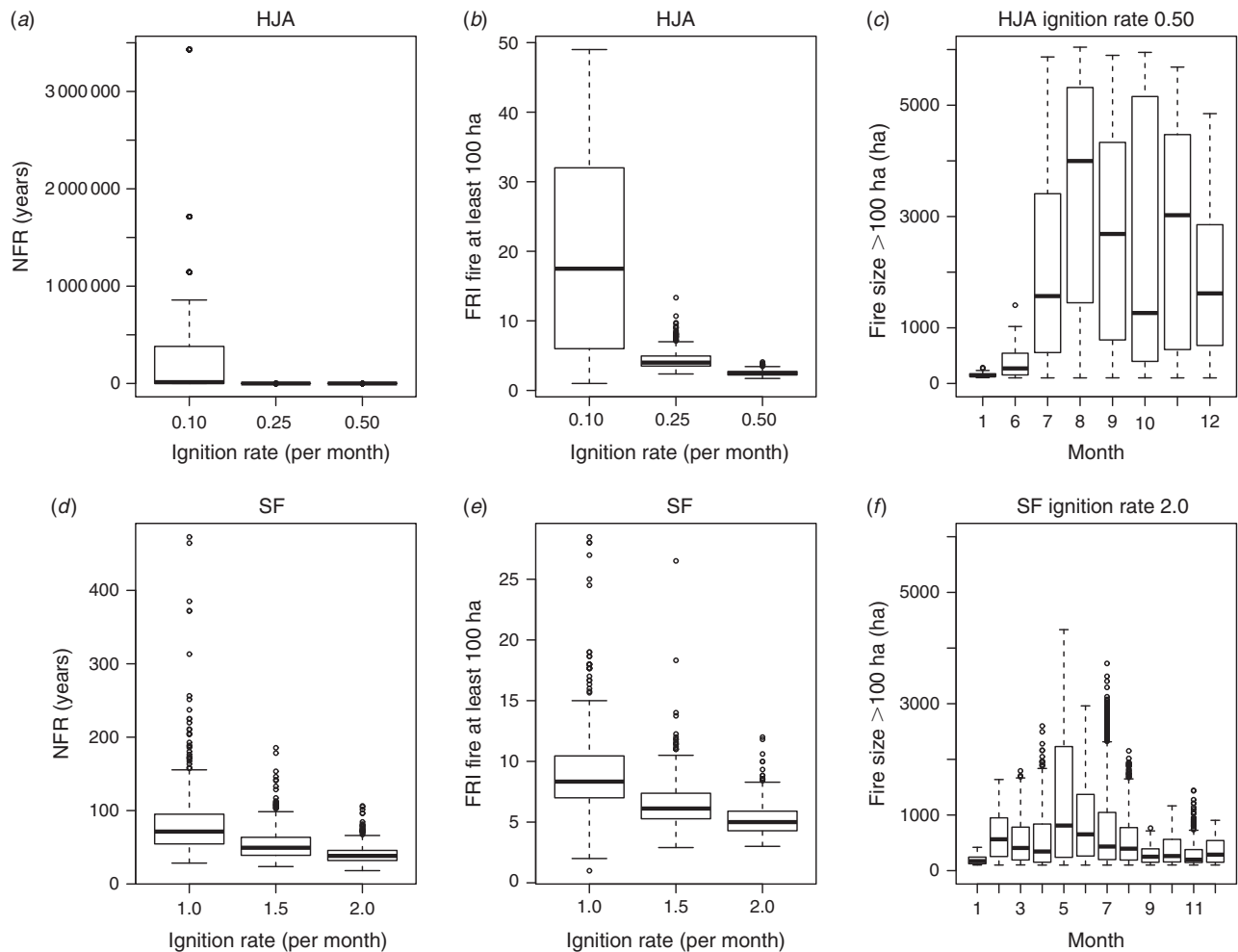


**Fig. 8.** Natural fire rotation, fire return intervals and fire size distributions (for fires that achieve a size  $>100$  ha) for (a–c) the HJ Andrews (HJA), and (d–f) Santa Fe (SF) watersheds. Source of variability is replicates (one value calculated per replicate simulation). Note different y axis scales between SF and HJA.

the third criterion for each watershed (fire frequency measured by return interval and NFR) is sensitive to the value of ignition source rate (Fig. 8). Therefore, some calibration of ignition source rates is necessary (as with some processes in the partner model RHESSys) to ensure that fire frequency *per se* is in line with historical observations. Our procedure is one level of abstraction (McKenzie and Perera 2015) above trying to replicate specific historical realisations of this stochastic process, in that our application niche is to characterise plausible distributions of the future rather than individual outcomes. As such, we believe it to be more robust to future projections, the principal goal of RHESSys–WMFire, than would be any attempt to model future changes in ignition rates.

#### WMFire prediction uncertainty

The sensitivity of fire frequency to ignition source rate is non-linear, with the strongest sensitivity at lower values of mean ignition source rate. An ignition source rate of 0.10 ignitions per month predicts a NFR and fire return interval that match fire history data and LANDFIRE data for HJA (Fig. 8), whereas

WMFire is able to match fire history and LANDFIRE data for SF with multiple values of ignition source rate. For SF, this results in a mean ignition test rate of  $0.00013$  to  $0.00026 \text{ ha}^{-1} \text{ month}^{-1}$  and for HJA, this results in a mean ignition test rate of  $0.000016 \text{ ha}^{-1} \text{ month}^{-1}$ . These values of mean ignition source rate do not scale consistently with watershed size, which indicates that there is some uncertainty in fire occurrence that is not explained by WMFire when integrated with RHESSys absent fire effects. These rates per hectare can help to narrow the calibration space when WMFire is applied to a new watershed in a similar vegetation type. To further calibrate the mean ignition source rate in a new watershed, the RHESSys–WMFire model should be run with multiple ignition source rates commensurate with those found here, and the rate that adequately matches expected patterns of fire occurrence should be chosen.

#### Future WMFire development and assessment

We designed WMFire to be a model of fire spread that balances model complexity with data input uncertainty. The model assessment presented here shows that with this balance, the model

is able to predict seasonality and spatial patterns of fire occurrence, with a documented uncertainty in model predictions of fire frequency that is associated with the mean ignition source rate.

The uncertainty in WMFire predictions of fire occurrence metrics such as fire return interval and NFR gives a pathway for improving the model integration. In WMFire, fire frequency predictions are sensitive to the mean ignition source rate, and the lower ignition source rate required for HJA may represent limitations in our current approach for estimating successful fire ignitions and spread. One possible limitation may be insufficient resolution of canopy structure because the current version of WMFire utilises a single integrated canopy in the estimation of deficit; however, in denser canopies, such as those in HJA, understorey deficit may be more relevant to the probability of fire start than the total vegetation as modelled here. Future work will explore this possibility.

The absence of fire effects in RHESSys means that the integration of WMFire and RHESSys is not yet fully bidirectional, in that RHESSys dynamically modifies fire spread, but the fire spread does not dynamically modify watershed characteristics. RHESSys is in the process of being updated to estimate fire effects. An important predictor of fire effects is the vertical stratification of the canopy fuels, with an understorey canopy acting as ladder fuels to the upper canopy. The increased resolution of canopy structure that will be implemented for fire starts can also be used to estimate canopy-level fire effects. In our third stage of model assessment, we will evaluate the improved simulation of fire starts with the fully coupled fire effects model against detailed fire regime characteristics for several watersheds in the western US. We then will determine the application niche of the fully bidirectional coupled ecohydrological and fire spread model.

## Acknowledgements

This work was funded by the US Geological Survey-sponsored Western Mountain Initiative, the US Forest Service Fire and Environmental Research Applications in the Pacific Northwest Research Station, and National Science Foundation Science, Engineering and Education for Sustainability Award Number 1520847. Robert Norheim, Carina Tapia and William Collier provided Geographic Information System consultation and map design. Data used to run the models, and the model results presented in this paper can be found at <https://dx.doi.org/10.6084/m9.figshare.3203938> (accessed 24 May 2017). Updated RHESSys code can be found at <https://github.com/RHESSys/RHESSys/wiki> (accessed 24 May 2017). The authors declare that they have no conflicts of interest.

## References

- Bartlein P, Hostetler S, Shafer S, Holman J, Solomon A (2008) Temporal and spatial structure in a daily wildfire-start data set from the western United States (1986–96). *International Journal of Wildland Fire* **17**, 8–17. doi:10.1071/WF07022
- Caldarelli G, Frondoni R, Gabrielli A (2001) Percolation in real wildfires. *Europhysics Letters* **56**, 510–516. doi:10.1209/EPL/I2001-00549-4
- Environmental Protection Agency (2009) Guidance on the development, evaluation, and application of environmental models. EPA/100/K-09/003/March2009. Available at <https://nepis.epa.gov/Exe/ZyPDF.cgi?Dockey=P1003E4R.PDF> [Verified 24 May 2017]
- Faivre NR, Jin Y, Goulden ML, Randerson JT (2016) Spatial patterns and controls on burned area for two contrasting fire regimes in southern California. *Ecosphere* **7**, e01210. doi:10.1002/ECS2.1210
- Fatichi S, Pappas C, Ivanov VY (2016) Modeling plant–water interactions: an ecohydrological overview from the cell to the global scale. *Wiley Interdisciplinary Reviews: Water* **3**, 327–368. doi:10.1002/WAT2.1125
- Finney MA (2004) FARSITE: Fire Area Simulator – Model development and evaluation. USDA Forest Service, Rocky Mountain Research Station, Research Paper RMRS-RP-4 Revised. (Fort Collins, CO, USA)
- Fiorucci P, Gaetani F, Minciardi R (2008) Regional partitioning for wildfire regime characterization. *Journal of Geophysical Research* **113**(F2), F02013. doi:10.1029/2007JF000771
- Flannigan MD, Krawchuk MA, de Groot WJ, Wotton MB, Gowman LM (2009) Implications of changing climate for global wildland fire. *International Journal of Wildland Fire* **18**, 483–507. doi:10.1071/WF08187
- Garcia ES, Tague CL (2015) Subsurface storage capacity influences climate – evapotranspiration interactions in three western United States catchments. *Hydrology and Earth System Sciences* **19**, 4845–4858. doi:10.5194/HESS-19-4845-2015
- Garcia ES, Tague CL, Choate JS (2013) Influence of spatial temperature estimation method in ecohydrologic modeling in the Western Oregon Cascades. *Water Resources Research* **49**, 1611–1624. doi:10.1002/WRCR.20140
- Hannah DM, Wood PJ, Sadler JP (2004) Ecohydrology and hydroecology: a ‘new paradigm’? *Hydrological Processes* **18**, 3439–3445. doi:10.1002/HYP.5761
- Hannah DM, Sadler JP, Wood PJ (2007) Hydroecology and ecohydrology: challenges and future prospects. In ‘Hydroecology and Ecohydrology: Past, Present and Future’. (Eds P Wood, DM Hannah, JP Sadler) pp. 421–429. (Wiley: Chichester, UK)
- Heinselman ML (1973) Fire in the virgin forests of the Boundary Waters Canoe Area, Minnesota. *Quaternary Research* **3**, 329–382. doi:10.1016/0033-5894(73)90003-3
- Hornberger G, Cosby B (1985) Selection of parameter values in environmental models using sparse data: a case study. *Applied Mathematics and Computation* **17**, 335–355. doi:10.1016/0096-3003(85)90040-2
- Hurteau MD, Bradford JB, Fulé PZ, Taylor AH, Martin KL (2014) Climate change, fire management, and ecological services in the south-western US. *Forest Ecology and Management* **327**, 280–289. doi:10.1016/J.FORECO.2013.08.007
- Hyde K, Dickinson MB, Bohrer G, Calkin D, Evers L, Gilbertson-Day J, Nicolet T, Ryan K, Tague C (2013) Research and development supporting risk-based wildfire effects prediction for fuels and fire management: status and needs. *International Journal of Wildland Fire* **22**, 37–50. doi:10.1071/WF11143
- Jackson LJ, Trebitz AS, Cottingham KL (2000) An introduction to the practice of ecological modeling. *Bioscience* **50**, 694–706. doi:10.1641/0006-3568(2000)050[0694:AITTPJ]2.0.CO;2
- Keane RE, Parsons RA, Hessburg PF (2002) Estimating historical range and variation of landscape patch dynamics: limitations of the simulation approach. *Ecological Modelling* **151**, 29–49. doi:10.1016/S0304-3800(01)00470-7
- Kennedy MC, McKenzie D (2010) Using a stochastic model and cross-scale analysis to evaluate controls on historical low-severity fire regimes. *Landscape Ecology* **25**, 1561–1573. doi:10.1007/S10980-010-9527-5
- Kennedy MC, McKenzie D (2017) Model evaluation identifies uncertainties and trade-offs in complexity when fire is integrated with hydro-ecological projections. In ‘Natural Hazard Uncertainty Assessment: Modelling and Decision Support’. (Eds K Riley, P Webley, M Thompson) American Geophysical Union Monograph Series, pp. 231–244. (American Geophysical Union: Washington, DC, USA)
- Krause A, Kloster S, Wilkenskeld S, Paeth H (2014) The sensitivity of global wildfires to simulated past, present, and future lightning frequency. *Journal of Geophysical Research. Biogeosciences* **119**, 312–322. doi:10.1002/2013JG002502



- LANDFIRE (2014) US Department of Interior, geological survey. Available at <http://landfire.cr.usgs.gov/viewer/> [Verified 2 March 2017].
- Littell JS, Oneil EE, McKenzie D, Hicke JA, Lutz JA, Norheim RA, Elsner MM (2010) Forest ecosystems, disturbance, and climatic change in Washington State, USA. *Climatic Change* **102**, 129–158. doi:10.1007/S10584-010-9858-X
- López-Moreno JI, Zabalza J, Vicente-Serrano SM, Revuelto J, Gilaberte M, Azorin-Molina C, Moran-Tejeda E, Garcia-Ruiz JM, Tague C (2014) Impact of climate and land-use change on water availability and reservoir management: scenarios in the Upper Aragón River, Spanish Pyrenees. *The Science of the Total Environment* **493**, 1222–1231. doi:10.1016/J.SCITOTENV.2013.09.031
- Malamud BD, Millington JDA, Perry GLW (2005) Characterizing wildfire regimes in the United States. *Proceedings of the National Academy of Sciences of the United States of America* **102**, 4694–4699. doi:10.1073/PNAS.0500880102
- Margolis EQ, Balmat J (2009) Fire history and fire–climate relationships along a fire regime gradient in the Santa Fe Municipal Watershed, NM, USA. *Forest Ecology and Management* **258**, 2416–2430. doi:10.1016/J.FORECO.2009.08.019
- McKenzie D, Kennedy MC (2012) Power laws reveal phase transitions in landscape controls of fire regimes. *Nature Communications* **3**, 726. doi:10.1038/ncomms1731
- McKenzie D, Perera A (2015) Modeling wildfire regimes in forest landscapes: abstracting a complex reality. In ‘Simulation Modeling of Forest Landscape Disturbances’. (Eds A Perera, B Sturdevant, L Buse) pp. 73–92. (Springer: New York, NY, USA)
- O'Neill R, Gardner R, Mankin J (1980) Analysis of parameter error in a non-linear model. *Ecological Modelling* **8**, 297–311. doi:10.1016/0304-3800(80)90043-5
- Reynolds JH, Ford ED (1999) Multicriteria assessment of ecological process models. *Ecology* **80**, 538–553. doi:10.1890/0012-9658(1999)080[0538:MCAOEP]2.0.CO;2
- Rocca ME, Brown PM, MacDonald LH, Carrico CM (2014) Climate change impacts on fire regimes and key ecosystem services in Rocky Mountain forests. *Forest Ecology and Management* **327**, 290–305. doi:10.1016/J.FORECO.2014.04.005
- Rothermel RC (1972) A mathematical model for predicting fire spread in wildland fuels. USDA Forest Service, Intermountain Forest and Range Experiment Station, Research Paper INT-116. (Odgen, UT, USA)
- Scott JH, Burgan RE (2005) Standard fire behavior fuel models: a comprehensive set for use with Rothermel's surface fire spread model. USDA Forest Service, Rocky Mountain Research Station, General Technical Report RMRS-GTR-153. (Fort Collins, CO, USA)
- Shakesby RA, Doerr SH (2006) Wildfire as a hydrological and geomorphological agent. *Earth-Science Reviews* **74**, 269–307. doi:10.1016/J.EARSCIREV.2005.10.006
- Stavros EN, Abatzoglou JT, McKenzie D, Larkin NK (2014) Regional projections of the likelihood of very large wildland fires under a changing climate in the contiguous western United States. *Climatic Change* **126**, 455–468. doi:10.1007/S10584-014-1229-6
- Stephenson N (1998) Actual evapotranspiration and deficit: biologically meaningful correlates of vegetation distribution across spatial scales. *Journal of Biogeography* **25**(5), 855–870. doi:10.1046/J.1365-2699.1998.00233.X
- Swann AL, Fung IY, Chiang JC (2012) Mid-latitude afforestation shifts general circulation and tropical precipitation. *Proceedings of the National Academy of Sciences of the United States of America* **109**, 712–716. doi:10.1073/PNAS.1116706108
- Swetnam T, Falk DA, Hessl AE, Farris C (2011) Reconstructing landscape pattern of historical fires and fire regimes. In ‘Landscape Ecology of Fire. Ecological Studies Vol. 213, Analysis and Synthesis’. (Eds D McKenzie, C Miller, D Falk) Ch. 7, pp. 165–192. (Springer: New York, NY, USA).
- Tague C, Band L (2004) RHESys: regional hydro-ecologic simulation system—an object-oriented approach to spatially distributed modeling of carbon, water, and nutrient cycling. *Earth Interactions* **8**, 1–42. doi:10.1175/1087-3562(2004)8<1:RRHSSO>2.0.CO;2
- Tague C, Dugger AL (2010) Ecohydrology and climate change in the mountains of the western USA—a review of research and opportunities. *Geography Compass* **4**, 1648–1663. doi:10.1111/J.1749-8198.2010.00400.X
- Tague CL, Choate JS, Grant G (2013a) Parameterizing subsurface drainage with geology to improve modeling streamflow responses to climate in data-limited environments. *Hydrology and Earth System Sciences* **17**, 341–354. doi:10.5194/HESS-17-341-2013
- Tague CL, McDowell NG, Allen CD (2013b) An integrated model of environmental effects on growth, carbohydrate balance, and mortality of *Pinus ponderosa* forests in the southern Rocky Mountains. *PLoS One* **8**, e80286. doi:10.1371/JOURNAL.PONE.0080286
- Teensma PDA (1987) Fire history and fire regimes of the Central Western Cascades of Oregon. PhD thesis, Oregon State University, Corvallis, OR, USA.
- Weisberg PJ (1998) Fire history, fire regimes, and development of forest structure in the Central Western Oregon Cascades. PhD thesis, Oregon State University, Corvallis, OR, USA.
- Weisberg PJ, Ko D, Py C, Bauer JM (2008) Modeling fire and landform influences on the distribution of old-growth pinyon–juniper woodland. *Landscape Ecology* **23**, 931–943. doi:10.1007/S10980-008-9249-0
- Wood PJ, Hannah DM, Sadler JP (2007) Ecohydrology and hydroecology: an introduction. In ‘Hydroecology and Ecohydrology: Past, Present and Future’. (Eds P Wood, DM Hannah, JP Sadler) pp. 1–6. (Wiley: Chichester, UK)
- Zierl B, Bugmann H, Tague CL (2007) Water and carbon fluxes of European ecosystems: an evaluation of the ecohydrological model RHESys. *Hydrological Processes* **21**, 3328–3339. doi:10.1002/HYP.6540